Improved Permeability Properties for Bacterial Cellulose/ Montmorillonite Hybrid Bionanocomposite Membranes by *In-Situ* Assembling

Itxaso Algar[1], Clara Garcia-Astrain[1], Alba Gonzalez[2], Loli Martin[3], Nagore Gabilondo[1], Aloña Retegi[1]*, and Arantxa Eceiza[1]*

[1] *Materials + Technologies Research Group, Polytechnic School, Department of Chemical and Environmental Engineering, University of the Basque Country, Plza. Europa 1, 20018, Donostia-San Sebastián, Spain*
[2] *POLYMAT, Department of Polymer Science and Technology, University of the Basque Country (UPV/EHU), 20080, Donostia-San Sebastián, Spain*
[3] *Macrobehavior-Mesostructure-Nanotechnology Service-SGIker (UPV/EHU), Polytechnic School, Department of Chemical and Environmental Engineering, University of the Basque Country, Plza. Europa 1, 20018, Donostia-San Sebastián, Spain*

Received October 27, 2015; Accepted January 05, 2016

ABSTRACT: Bacterial cellulose/montmorillonite (BCMMT) hybrid bionanocomposite membranes were prepared by *in-situ* assembling or one-step biosynthesis process. The presence of MMT in BC membranes was confirmed by thermogravimetric analysis and quantified by mass spectrometry, resulting in bionanocomposites with MMT contents between 7–13 wt%. The incorporation of MMT during BC biosynthesis modified BC morphology and led to lower porosity, even though higher water holding capacity was achieved. Bionanocomposites showed improved thermal stability and water vapor and oxygen gas barrier properties up to 70 and 80% with respect to neat BC membranes. This improvement was related to the tortuous path of gas diffusion created by MMT nanoplatelets due to the high extent of dispersion achieved, as observed by XRD. SEM micrographs confirmed MMT was finely dispersed between BC nanofibrils and a more compact structure was observed as MMT content increased. Thus, the *in-situ* process can be used as an alternative method to obtain cellulose/MMT hybrid bionanocomposite that would have potential applications as reinforcing element.

KEYWORDS: Bacterial cellulose, composite materials, *in-situ* biosynthesis, montmorillonite, permeability, thermogravimetric analysis

1 INTRODUCTION

In the last decade, due to environmental concerns and sustainability awareness, there has been a growing interest in developing materials and technologies that can reduce dependence on petroleum. In this aspect, the so-called green materials can meet the needs of new emerging fields [1–5]. Bionanocomposites with added functional properties can provide high value materials' requirements, suitable for biomedical engineering and food packaging applications, among others [6–10]. These high value materials present improved mechanical, thermal, barrier or fire retardancy properties without losing their environmental friendliness [11–13].

*Corresponding authors: arantxa.eceiza@ehu.es; alona.retegui@ehu.es
DOI: 10.7569/JRM.2015.634124

Bionanocomposites are comprised of a naturally occurring biopolymer matrix reinforced with small quantities of nanoentities having high aspect ratios and at least one dimension in the nanometric scale (1–100 nm) [14]. Bacterial cellulose (BC) is an interesting matrix for the preparation of bionanocomposites due to its excellent physicochemical and mechanical properties, biodegradability and the ultrafine 3D network-like structure [15]. Synthesized by bacteria as a mechanism of protection, the produced BC membranes possess high crystallinity, water uptake ability and mechanical strength in the wet state [16]. Moreover, BC has been widely used for biomedical and food packaging applications due to its great stability, low toxicity, non-allergenicity, and, it can be adequately sterilized [17]. In addition, BC exhibits much higher mechanical properties than other biodegradable polymers like gelatin or chitosan, among others [18]. Since the first BC composites prepared

by Gindl and Keckes from BC/acetate butyrate by means of solvent casting evaporation, several composite preparation strategies have been investigated [19]. Zhijiang *et al.* prepared porous scaffolds based on poly(3-hydroxybutyrate-co-4-hydroxybutyrate) and BC by freeze-drying and obtained bioactive biocomposites for biomedical applications [20]. Thus, the porous structure of the three-dimensional network formed by BC can accommodate various hosts for use in various applications. An alternative can be found in mineral nanoclays. Montmorillonite (MMT) is one of the most common clay minerals of the smectite family, which is of interest as reinforcing material in food packaging applications [21]. By the addition and good dispersion (without agglomerates) of MMT, thermal stability, barrier properties and mechanical properties of the nanocomposites can be improved. Thus, several procedures have been used to obtain well-dispersed systems. Ul-Islam *et al.* prepared bacterial cellulose-MMT composites by impregnation of BC sheets with MMT dispersions, aiming to obtain composites possessing inherited antibacterial, wound healing and drug-carrying properties [22]. Liu and Berglund prepared nanopaper structures with high MMT content from a chitosan solution with MMT and nanofibrillated cellulose, obtaining improved mechanical and oxygen barrier properties, and also fire retardancy [23]. However, *ex-situ* fabrication technologies are lengthy and tedious and therefore other alternative processes are necessary. BC-based composites can be obtained by *in-situ* polymerization or a one-step method, which consist on the addition of some additives to the culture medium. However, depending on the additives' nature, their incorporation can affect cellulose production, interfering with crystallization and consequently changing the properties of BC such as yield, structure, morphology and physicochemical properties [24, 25]. Grande *et al.* prepared BC/hydroxyapatite composites for use in biomedical applications by *in-situ* modification, using carboxymethyl cellulose to improve the dispersion of hydroxyapatite, and they observed great changes in the properties of the obtained cellulose such as a 50% diameter reduction, lower crystallinity and higher porosity [26].

The aim of the present study is the fabrication of BCMMT bionanocomposites with different MMT contents by *in-situ* polymerization method and to study the effect of MMT incorporation on the thermal, morphological and barrier properties. The incorporation of MMT was analyzed and quantified by thermal analysis and mass spectrometry and was also confirmed by SEM. Moreover, the effect of the MMT incorporation on the crystallinity, determined by XRD analysis, water holding capacity and water and oxygen barrier properties, analyzed by means of permeability measurements, was investigated.

2 EXPERIMENTAL SECTION

2.1 Materials

Unmodified MMT supplied by Nanocor, Inc. (Nanomer PGV) with cation exchange capacity (CEC) of 145 ± 10 eq/100 g clay was used as received. BC and their hybrid bionanocomposites were prepared in our laboratory using household wastes as growing medium.

2.2 BCMMT Biosynthesis

In order to obtain BCMMT hybrid bionanocomposites, first of all, MMT/water dispersions containing 0.5, 1 and 2 wt% MMT were prepared by ultrasonication (Bioblock Scientific Vibra Cell™ 75043) at a maximum of 750 W and an amplitude of 20% during 60 min (Figure 1a). The resulting dispersion was incorporated into BC growing medium and after incubation at 28 °C during 13 days in static culture conditions, BCMMT membranes were obtained. In order to remove cells and other impurities, the obtained BCMMT membranes with a thickness of 0.5–0.7 cm were boiled in 2 wt% KOH solution for 24 h, and thereafter thoroughly washed with water until total neutralization to obtain BCMMT hybrid membranes with different MMT contents (Figure 1b). As reference a BC membrane without MMT was prepared (Figure 1c), following the same protocol as for BCMMT membranes and published in a previous work [27].

2.3 BCMMT Films Preparation

The BC and BCMMT films were prepared by compression from their corresponding membranes, using a hydraulic press at 60 °C for 5 min and 10 MPa to squeeze out any remaining water. Samples were stored in a desiccator before characterization. The different BCMMT hybrid membranes and films were named as BCMMTX, where X denotes the amount (expressed as weight percent) of MMT in the final composite, determined by laser ablation inductively coupled plasma mass spectrometry (LA-ICP-MS).

2.4 Characterization

2.4.1 MMT Content

MMT content in the obtained BCMMT films was determined by measuring the amount of Si element,

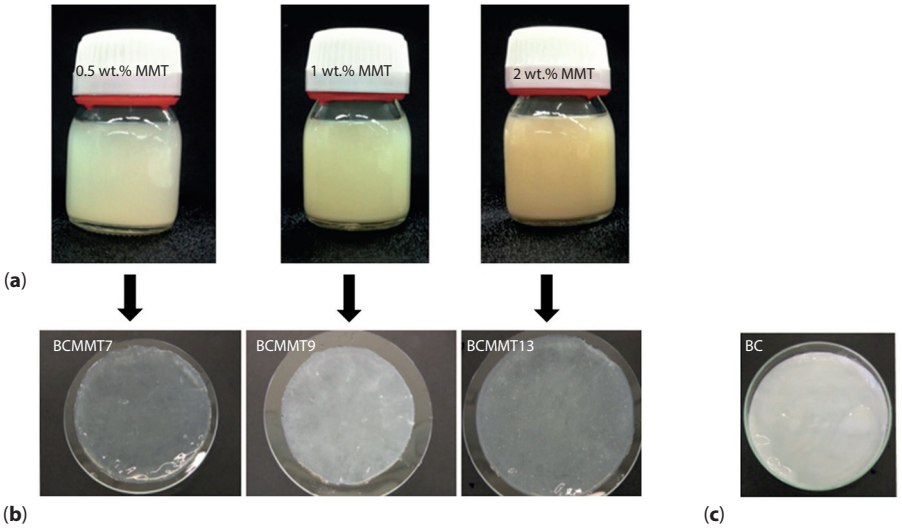

Figure 1 Photographs and visual appearance of: (**a**) MTT dispersions prepared by ultrasonication containing 0.5, 1 and 2 wt% of MMT, (**b**) Purified BCMMT membranes containing 7, 9 and 13 wt% of MMT and (**c**) a BC membrane without MMT as reference.

using a LA-ICP-MS, Agilent Technologies 7500ce model. A nebulizer and spray chamber PFA to avoid interferences with an internal diameter of 2.5 mm was used. Before LA-ICP-MS analysis, samples were digested by immersing them in an acidic mixture (nitric, hydrofluoric and boric acids) and then heating in a microwave system at 200 °C and maximum power.

2.4.2 *Porosity Measurements*

Porosity of BC and BCMMT films was determined using the following equation [28]:

$$\text{Porosity} = \left(1 - \frac{\rho_f}{\rho_t}\right) \times 100 \quad (1)$$

where ρ_t is the theoretical density of films, predicted using density mixing rule, and ρ_f is the film density calculated in an Archimedes balance using benzene (ρ = 0.870 g mL^{-1}) as a solvent. Three samples of each system were tested.

2.4.3 *Water Holding Capacity*

Previous to water holding capacity (*WHC*) measurements, BC samples were freeze-dried and vacuum dried (W_{dry}). Thereafter, BC samples were immersed in deionized water until a constant weight was reached, rehydrate weight (W_{wet}). Three samples of each system were tested. The *WHC* was calculated with the following equation:

$$WHC(\%) = \left(\frac{W_{wet} - W_{dry}}{W_{dry}}\right) \times 100 \quad (2)$$

2.4.4 *Thermogravimetric Analysis*

Thermogravimetric analysis (TG) was performed to analyze the moisture content and thermal stability of BCMMT hybrid bionanocomposites using TGA/SDTA 851 Mettler Toledo equipment. Tests were carried out from room temperature to 800 °C at a scanning rate of 5 °C/min under oxygen atmosphere. The weight loss thermograms and their derivative curves (DTG) were analyzed. From the obtained results, the evaporated water content, the onset temperature of weight loss (T_{onset}), the temperature of maximum weight loss (T_{max}) and the residue content at 800 °C were determined.

2.4.5 *Scanning Electron Microscopy*

Scanning electron microscopy (SEM) was used to analyze the morphology of biosynthesized BC and the location and dispersion of MMT in the membranes. Previous to performing SEM analysis, samples were freeze-dried. The lyophilized samples were coated with gold/palladium using an ion sputter coater and afterwards observed with a Jeol JSM-6400 scanning microscope operating at 20 kV.

2.4.6 *X-Ray Diffractometry*

X-ray diffractometry (XRD) technique was used to analyze the crystalline structure of BC samples and also to study MMT intercalation/exfoliation in BCMMT samples. X-ray diffraction patterns were measured using a X-ray diffractometer PW1710 (Philips) with CuKα radiation (λ = 1.54 Å). The diffraction data were collected from 2θ values from 10° to 40°, with a step size of 0.02 and 1.25 s times per step. The crystallinity

index (*CI*) of BC films was calculated from the reflected intensity data using the method of Segal *et al*. [29]:

$$CI = \frac{I_{020} - I_{am}}{I_{020}} \quad (3)$$

where I_{020} is the maximum intensity of the lattice diffraction, and I_{am} is the intensity at 2θ = 18°.

2.4.7 Barrier Properties

Water vapor transmission rate (WVTR) measurements were carried out at 25 °C according to ASTM E96-95 standard [30], using a permeation gravimetric cell placed on a Sartorius balance with a readability of 10^{-5} g. The cell was filled with water (water activity = 1, pure water) and covered with the bionanocomposite film, so the difference in concentration at each side of the film generated a weight loss on the cell related with the water vapor transmission, which was monitored and recorded in a computer for further data treatment.

WVTR was calculated from the following equation:

$$WVTR = \frac{m \times l}{A \times (a_{in} - a_{out})} \quad (4)$$

where m is the mass, l is the film thickness, A is the film area (2.54 cm^2) and a_{in} and a_{out} are the relative humidity inside and outside the cell. Film thickness was measured by a Duo-Check gauge, with an accuracy of 1 µm. The results reported are the average of at least three measurements.

The oxygen permeability measurements were carried out using a MOCON OX-TRAN Model 2/21 gas permeability tester in accordance with the ASTM standard D3985-10 [31]. The oxygen transmission rate (OTR) through BC and BCMMT bionanocomposites was tested at 760 mmHg, 50% relative humidity and 23 °C. Three samples of each system were tested.

3 RESULTS AND DISCUSSION

3.1 MMT Content, Porosity and WHC

First, the real MMT content of BCMMT films was calculated by LA-ICP-MS. As can be seen in Table 1, the real MMT content of BCMMT films obtained from 0.5, 1 and 2 wt% MMT dispersions is 7, 9 and 13 wt% respectively. No dispersions with higher percentages of MMT were used because MMT precipitated in the medium. It can be observed that as MMT content increases in the dispersion, the higher the percentage of MMT in the final composite is. Yan *et al*. obtained similar results for BC/multiwalled carbon nanotubes (MWNT) in agitated culture medium where higher MWNT content was incorporated into the composites as the MWNT content in the medium increases [32]. Porosity decreases with the incorporation of MMT into BC membranes, only slightly (from 12.03 ± 0.04 to 11.83 ± 0.33) for the lowest amount of MMT but up to 50% (6.33 ± 0.07) for the highest amount. These results suggest that due to the addition of MMT and its suitable dispersion, MMT clays are captured in BC nanofibrils, resulting in a more compact structure. WHC of BC and BCMMT hybrid films was also analyzed, resulting in a higher WHC as MMT content increases. Although the hydrophilic nature of cellulose and the high water retention capacity of BC are known, the addition of MMT (also hydrophilic) allows the obtainment of higher WHC values compared to neat BC membranes.

Table 1 MMT content, porosity, water holding capacity and crystallinity index of BC and BCMMT bionanocomposites.

System	MMT content (wt%)	Porosity (%)	WHC (%)	CI (%)
BC	0	12.03 ± 0.04	692 ± 81	84.9
BCMMT7	7	11.83 ± 0.33	1923 ± 197	83.8
BCMMT9	9	9.87 ± 0.70	2653 ± 6	84.4
BCMMT13	13	6.33 ± 0.07	3460 ± 144	76.7

3.2 Crystallinity Analysis

The incorporation of MMT during the biosynthesis of BC can affect cellulose production due to the fact that assembly of cellulose is influenced by chemical and physical parameters and is supposed to change the crystallization process of cellulose. The XRD technique is an adequate tool to study the arrangement of cellulose molecules and its crystallinity. Besides that, XRD is used to analyze intercalated and exfoliated structures in MMT-based nanocomposites. The XRD pattern of neat BC shows reflections at around 14.5° and 22.7°, characteristic of the typical profile of cellulose I allomorph biosynthesized in static culture (Figure 2) [27]. In the XRD pattern of MMT, a reflection of about 7.1° can be observed, which corresponds to a basal spacing of 1.25 nm, estimated from Bragg's equation [33–35]. This is in agreement with the d-spacing value of 1.22 nm provided by the supplier. The almost total absence of this reflection for BCMMT hybrid bionanocomposites suggests that MMT layers show adequate dispersion with a high extent of intercalation/exfoliation. As reported, the multilayer structure of the clay mineral is maintained in an intercalated nanocomposite, so its interlayer basal spacing

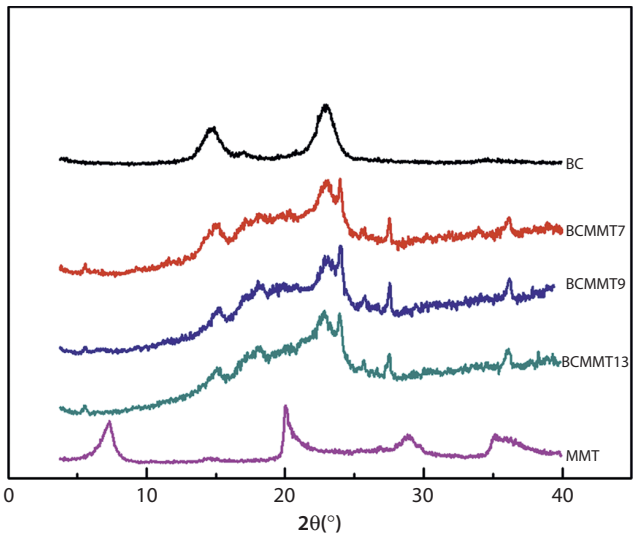

Figure 2 X-ray diffraction patterns of the BC and BCMMT films and MMT.

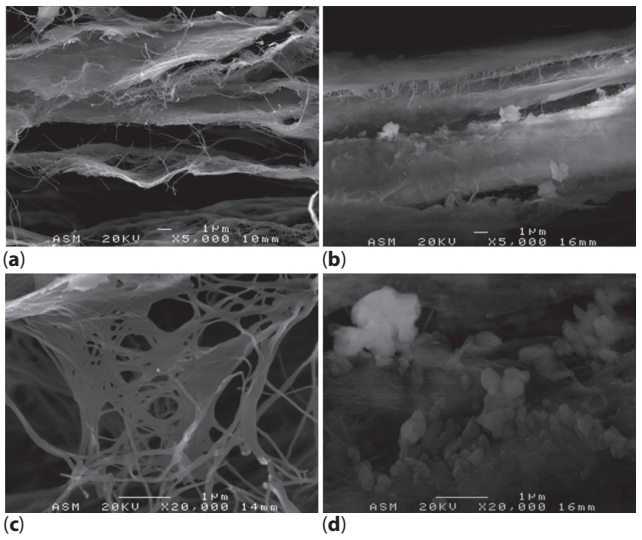

Figure 3 (**a**, **b**) SEM images (x5000) of lyophilized BC and BCMMT9 membranes cross section (bar scale 1 μm); (**c**, **d**) SEM images (x20000) of lyophilized BC and BCMMT9 membranes cross section (bar scale 1 μm).

can be estimated. Intercalated polymer chains usually increase the interlayer basal spacing of the clay, leading to a shift of the reflection towards lower angle values [36]. On the contrary, in an exfoliated nanocomposite, reflection of the clay mineral disappears from the XRD patterns due to lack of order between the silicate layers [37, 38]. Liu and Berglund prepared a multilayered nacre-like nanopaper structure based on MMT and cellulose nanofibers by using chitosan to encourage the dispersion of MMT by mechanical mixing [23]. An increase of the interlayer distance was observed by XRD, indicating that chitosan was intercalated into the interlayers of MMT, however, exfoliated structures were not observed. Ul-Islam *et al.* prepared BCMMT composites by impregnation of BC sheets with MMT dispersions and observed a peak around 8–9° in all BCMMT XRD patterns, indicating that MMT was present, and only a decrease in intensity or a shifting to lower angles was detected [22]. This behavior was related to partial delamination of interplanar layers of clay mineral particles. Thus, taking into account the obtained results, it can be concluded that the incorporation of MMT during the BC biosynthesis process provides an improvement over the MMT composites preparation, due to the fact that a high extent of dispersion was achieved. However, electron microscopy techniques seem necessary to support those results.

The crystallinity index (CI) values calculated from XRD patterns are shown in Table 1. The CI of neat BC is 84.9%, and although it decreases slightly for BCMMT7 and BCMMT9, they still maintain a high value of crystallinity index, whereas it decreases up to 76.7% for BCMMT13 bionanocomposite. This is further evidence that MMT has a great impact on the biosynthesis of cellulose. This trend is in accordance with previous studies which showed that additives in the growing medium usually decrease the overall crystallinity of BC. Ruka *et al.* prepared a fully degradable nanocomposite system based on poly-3-hydroxybutyrate (PHB) and bacterial cellulose by *in-situ* modification method and observed a drastic decrease in crystallinity [39]. As reported by other authors, *in-situ* modified BC nanocomposites show lower crystallinity values due to interactions between sub-elementary bacterial cellulose fibrils and the additives incorporated into the medium during biosynthesis [24].

3.3 Morphology Analysis

SEM analysis is a complementary technique to XRD for characterizing the nanocomposite structure. Figure 3 shows the cross section of neat BC and BCMMT hybrid (BCMMT9) membranes. In the case of neat BC (Figure 3a and 3c), loosely packed cellulose nanofibrils forming different cellulose layers can be observed, whereas a more compact structure is observed in the BCMMT hybrid membrane (Figure 3b and 3d); also, MMT nanolayers can be observed over BC nanofibrils. Moreover, the compactness of the cross section is clearly different (Figure 3a and 3b), in agreement with the lower porosity values obtained for hybrid films with respect to neat BC. As can be observed, it seems that cellulose nanofibers are enveloped by MMT nanosheets.

3.4 Thermal Stability

The thermal stability of BC and BCMMT hybrid films was studied by thermogravimetric analysis. In addition, thermal degradation can be related to material composition (BC and MMT) owing to their different thermal behavior [40]. The thermal degradation of MMT shows a weight loss in the range of 25–100 °C, which is related to adsorbed water due to its hydrophilic nature. Besides that, due to the high mineral content of MMT (up to 70 wt%), it exhibits high thermal stability up to 600 °C, with a char residue higher than 93 wt% related to the hydrated MMT and up to 99 wt% after water removal (Figure 4). Thermal degradation of BC involves dehydration (80–120 °C), depolymerization (250–400 °C) and decomposition of glycosyl units (> 400 °C) [41] (Figure 4). Regarding BCMMT hybrid bionanocomposites, they show the same degradation steps observed for BC (Figure 4). Table 2 reports the weight loss related to moisture content, onset and maximum depolymerization temperatures, T^1onset and T^1max, onset and maximum decomposition of glycosyl units, T^2onset and T^2max, and residue content at 800 °C. Moisture content of BCMMT hybrid bionanocomposites decreases as MMT content increases. BCMMT hybrids show improved thermal stability compared to neat BC. The onset and maximum degradation temperatures of both steps, the depolymerization and the decomposition of glycosyl units, increase as MMT content increases. As reported by other authors, the presence of MMT sheets can protect cellulose against thermal shock [22]. The sheets act as a heat barrier, providing hindrance to the diffusion of heat and mass transfer to the surface, thus retarding the decomposition rate [42]. Moreover, according to porosity values and SEM images, the compactness of BCMMT sample is higher than neat BC, thus delaying gas diffusion through the sample. Also, under oxidative conditions the degradation step occurred at comparable temperatures but the charring significantly increased for BCMMT bionanocomposites, from 0 to a maximum 13% at 800 °C. Furthermore, the residue observed in the hybrid bionanocomposites could be due to the high char formation capacity of MMT increasing as MMT content increases.

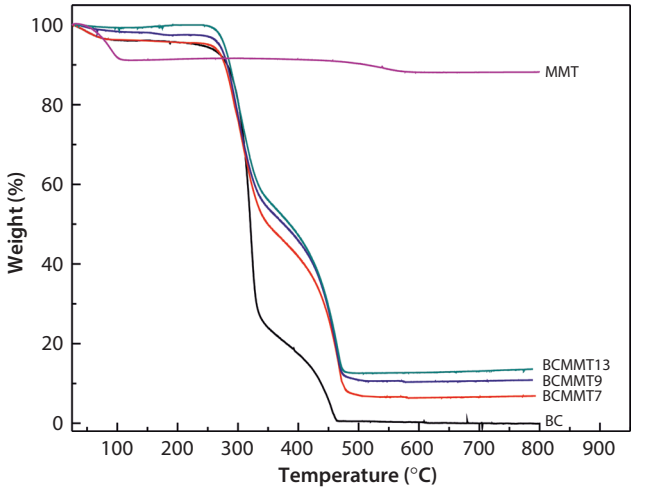

Figure 4 TG curves of BC and BCMMT films and MMT.

3.5 Barrier Properties

As reduction in water and oxygen permeability is desirable for potential application of BC membranes in packaging, the effect of MMT incorporation on the barrier properties was analyzed (Table 3). As can be observed, the incorporation of MMT reduces the films' water vapor and oxygen gas transmission rate. The WVTR values of BC membranes decreases with the presence of MMT, thus WVTR is reduced by as much as 70% as the MMT content increased from 0% to 9%. The higher WVTR of BCMMT13 bionanocomposite could be related to the decrease of crystallinity. The oxygen permeability is a key parameter in the study of permeability of gases in films for packaging, since the oxygen causes oxidation. In this case, analyzing OTR results, the same trend observed for water vapor has been observed. The incorporation of MMT into BC causes a sharp drop of the OTR with a reduction of about 80% in all BCMMT bionanocomposites. The reduction in both WVTR and OTR has been attributed

Table 2 Moisture content, onset and maximum depolymerization temperatures, T^1onset and T^1max, onset and maximum decomposition of glycosyl units T^2_{onset} and T^2_{max}, and residue content from TG and DTG curves of neat BC and BCMMT bionanocomposites.

System	Moisture content (%)	Temperature (ºC)				Residue (%)
		T^1_{onset}	T^1_{max}	T^2_{onset}	T^2_{max}	
BC	4.0	220	317	387	449	0
BCMMT7	3.6	234	305	390	463	7
BCMMT9	1.8	242	298	393	457	11
BCMMT13	1.0	243	303	395	458	13

Table 3 Water vapor and oxygen transmission rates of BC and BCMMT bionanocomposites.

System	WVTR (g mm/ m^2 day)	OTR (cm^3 mm/m^2 day atm)
BC	22.8 ± 0.3	0.28 ± 0.020
BCMMT7	6.6 ± 0.4	0.051 ± 0.001
BCMMT9	5.4 ± 2.5	0.041 ± 0.002
BCMMT13	15.6 ± 4.5	0.041 ± 0.003

to the creation of a tortuous pathway for the gas to diffuse through the nanocomposite. While tortuosity is usually the primary mechanism by which clay mineral sheets modify the nanocomposites' barrier properties, in this case other factors must be taken into account. As observed previously, the WHC of BC membranes increases with MMT content due to the hydrophilic nature of MMT. Furthermore, MMT interferes with BC biosynthesis modifying the free volume and porosity in the three-dimensional structure of BC nanofibrils, as confirmed by SEM images. The combination of tortuosity, increase of WHC and reduced porosity as a consequence of the high extent of intercalated/exfoliated MMT resulted in trapped water vapor and oxygen molecules in BCMMMT films. As observed in X-ray diffractograms and SEM images, the *in-situ* method favors MMT dispersion into BC matrix, contributing to a decrease in permeability. Yeh *et al*. showed that when MMT platelets were present during the *in-situ* polymerization of poly(methylmethacrylate) (PMMA), the obtained nanocomposites showed better MMT exfoliation and improved barrier properties against oxygen and water in comparison to MMT/PMMA composites prepared by solution dispersion [43]. Likewise, reductions of around 75 and 85% in OTR and 71 and 78% in WVTR, both at 50% of relative humidity, were reported for biohybrid films containing 10 and 20 wt% of highly exfoliated vermiculite nanoplatelets homogeneously distributed within a nanofibrillated cellulose matrix, respectively, highlighting the importance of the extremely tortuous pathway created by highly exfoliated nanostructures [44].

4 CONCLUSIONS

In this work, BCMMT hybrid bionanocomposites with high MMT content have been prepared by *in-situ* assembling process. The incorporation of MMT during BC biosynthesis has been confirmed by mass spectrometry and thermogravimetric analysis, and hybrid bionanocomposites containing 7, 9 and 13 wt% of MMT have been prepared. Hybrid bionanocomposites have shown lower WVTR and OTR values due to a combination of tortuosity, reduced porosity and higher water holding capacity induced by the finely dispersed MMT through BC membrane. In this work, hybrid BCMMT membranes have been obtained by a one-step process, which can be considered an alternative and efficient method for obtaining BC-based nanocomposites with potential applications in packaging, due to their improved barrier properties.

ACKNOWLEDGMENTS

The authors acknowledge the financial support from the Basque Country Government in the frame of Grupos Consolidados IT 776-13, from the University of the Basque Country (UPV/EHU) (EHUA12/19), from the Foundation Domingo Martínez (2015-Área Materiales 2) and from the Spanish Ministry of Economy and Competitiveness (MINECO) (MAT2013-43076-R). Additionally, I.A. thanks the UPV/EHU for the PhD fellowship (PIF10/2010/PIF10053). The authors are also grateful to the Macrobehavior-Mesostructure-Nanotechnology SGIker unit of the UPV/EHU for their technical support.

REFERENCES

1. T.A. Hottle, M.M. Bilec, and A.E. Landis, sustainability assessments of bio-based polymers. *Polym. Degrad. Stab.* **98**, 1898–1907 (2013). doi: 10.1016/j.polymdegradstab.2013.06.016.
2. S. Laurichesse and L. Avérous, Chemical modification of lignins: Towards biobased polymers. *Progr. Polym. Sci.* **39**, 1266–1290 (2013). doi: 10.1016/j.progpolymsci.2013.11.004.
3. M.R. Yates and C.Y. Barlow, Life cycle assessments of biodegradable, commercial biopolymers: A critical review. *Resour. Conserv. Recy.* **78**, 54–66 (2013). doi: 10.1016/j.resconrec.2013.06.010.
4. J.W. Rhim, H.M. Park, and C.S. Ha, Bio-nanocomposites for food packaging applications. *Prog. Polym. Sci.* **38**, 1629–1652 (2013). doi: 10.1016/j.progpolymsci.2013.05.008.
5. J.C. Ronda, G. Lligadas, M. Galià, and V. Cádiz, A renewable approach to thermosetting resins. *React. Funct. Polym.* **73**, 381–395 (2013). doi: 10.1016/j.reactfunctpolym.2012.03.015.
6. M. Alboofetileh, M. Rezaei, H. Hosseini, and M. Abdollahi, Effect of montmorillonite clay and biopolymer concentration on the physical and mechanical properties of alginate nanocomposite films. *J. Food Eng.* **117**, 26–33 (2013). doi: 10.1016/j.jfoodeng.2013.01.042.
7. M.C. Cruz-Romero, T. Murphy, M. Morris, E. Cummins, and J.P. Kerry, Antimicrobial activity of chitosan, organic acids and nano-sized solubilisates for potential use in smart antimicrobially-active packaging for potential

food applications. *Food Control* **34** 393–397 (2013). doi: 10.1016/j.foodcont.2013.04.042.
8. M. Ghaderi, M. Mousavi, H. Yousefi, and M. Labbafi, All-cellulose nanocomposite film made from bagasse cellulose nanofibers for food packaging application. *Carbohydr. Polym.* **104**, 59–65 (2014). doi: 10.1016/j.carbpol.2014.01.013.
9. T. Hirvikorpi, M. Vähä-Nissi, A. Harlin, M. Salomäki, S. Areva, J.T. Korhonen, and M. Karppinen, Enhanced water vapor barrier properties for biopolymer films by polyelectrolyte multilayer and atomic layer deposited Al_2O_3 double-coating. *Appl. Surf. Sci.* **257**, 9451–9454 (2011). doi: 10.1016/j.apsusc.2011.06.031.
10. P. Kanmani and J.W. Rhim, Properties and characterization of bionanocomposite films prepared with various biopolymers and ZnO nanoparticles. *Carbohydr. Polym.* **106**, 190–199 (2014). doi: 10.1016/j.carbpol.2014.02.007.
11. S. Alix, A. Mahieu, C. Terrie, J. Soulestin, E. Gerault, M.G.J. Feuilloley, R. Gattin, V. Edon, T. Ait-Younes, and N. Leblanc, Active pseudo-multilayered films from polycaprolactone and starch based matrix for food-packaging applications. *Eur. Polym. J.* **49**, 1234–1242 (2013). doi: 10.1016/j.eurpolymj.2013.03.016.
12. A. Liu, A. Walther, O. Ikkala, L. Belova, and L.A. Berglund, Clay nanopaper with tough cellulose nanofiber matrix for fire retardancy and gas barrier functions. *Biomacromolecules* **12**, 633–641 (2011). doi: 10.1021/bm101296z.
13. J. Wang and Z. Mao, Modified montmorillonite and its application as a flame retardant for polyester. *J. Appl. Polym. Sci.* **131**, 3516–3523 (2014). doi: 10.1002/app.39625.
14. E. Manias, A. Touny, L. Wu, K. Strawhecker, B. Lu, and T.C. Chung, Polypropylene/montmorillonite nanocomposites. Review of the synthetic routes and materials properties. *Chem. Mater.* **13**, 3516–3523 (2001). doi: 10.1021/cm0110627.
15. M. Iguchi, S. Yamanaka, and A. Budhiono, Bacterial cellulose–a masterpiece of nature's arts. *J. Mater. Sci.* **35**, 261–270 (2000). doi: 10.1023/A:1004775229149.
16. W. Czaja, A. Krystynowicz, S. Bielecki, and R.M. Brown Jr., Microbial cellulose–the natural power to heal wounds. *Biomaterials* **27**, 145–151 (2006). doi:10.1016/j.biomaterials.2005.07.035.
17. W.C. Lin, C.C. Lien, H.J. Yeh, C.M. Yu, and S.H. Hsu, Bacterial cellulose and bacterial cellulose–chitosan membranes for wound dressing applications. *Carbohydr. Polym.* **94**, 603–611 (2013). doi: 10.1016/j.carbpol.2013.01.076.
18. W. Yao, X. Wu, J. Zhu, B. Sun, Y.Y. Zhang, and C. Miller, Bacterial cellulose membrane – A new support carrier for yeast immobilization for ethanol fermentation. *Process Biochem.* **46**, 2054–2058 (2011). doi: 10.1016/j.procbio.2011.07.006.
19. W. Gindl and J. Keckes, Tensile properties of cellulose acetate butyrate composites reinforced with bacterial cellulose. *Comp. Sci. Technol.* **64**, 2407–2413 (2004). doi: 10.1016/j.compscitech.2004.05.001.
20. C. Zhijianga, H. Chengwei, and Y. Guang, Poly(3-hydroxubutyrate-co-4-hydroxubutyrate)/bacterial cellulose composite porous scaffold: Preparation, characterization and biocompatibility evaluation. *Carbohydr. Polym.* **87**, 1073–1080 (2013). doi:10.1016/j.carbpol.2011.08.037.
21. H.M. Park, X. Li, C.Z. Jin, C.Y. Park, W.J. Cho, and C.S. Ha, Preparation and properties of biodegradable thermoplastic starch/clay hybrids. *Macromol. Mater. Eng.* **287**, 553–558 (2002). doi: 10.1002/1439-2054(20020801).
22. M. Ul-Islam, T. Khan, and J.K. Park, Nanoreinforced bacterial cellulose-montmorillonite composites for biomedical applications. *Carbohydr. Polym.* **89**, 1189–1197 (2012). doi.org/10.1016/j.carbpol.2012.03.093.
23. A. Liu and L.A. Berglund, Clay nanopaper composites of nacre-like structure based on montmorrilonite and cellulose nanofibers–Improvements due to chitosan addition. *Carbohydr. Polym.* **87**, 53–60 (2012). doi:10.1016/j.carbpol.2011.07.019
24. K.C. Cheng, J.M. Catchmark, and A. Demirci, Effect of different additives on bacterial cellulose production by Acetobacter xylinum and analysis of material property. *Cellulose* **16**, 1033–1045 (2009). doi: 10.1007/s10570-009-9346-5.
25. L.L. Zhou, D.P. Sun, L.Y. Hu, Y.W. Li, and J.Z. Yang, Effect of addition of sodium alginate on bacterial cellulose production by Acetobacter xylinum. *J. Ind. Microbiol. Biotechnol.* **34**, 483–489 (2007). doi: 10.1007/s102925-007-0218-4.
26. C.J. Grande, F.G. Torres, C.M. Gomez, and M.C. Bañó, Nanocomposites of bacterial cellulose/hydroxyapatite for biomedical applications. *Acta Biomater.* **5**, 1605–1615 (2009). doi: 10.1016/j.actbio.2009.01.022.
27. I. Algar, S.C.M. Fernandes, G. Mondragon, C. Castro, C. Garcia-Astrain, N. Gabilondo, A. Retegi, and A. Eceiza, Pineapple agroindustrial residues for the production of high value bacterial cellulose with different morphologies. *J. Appl. Polym. Sci.* **132**, 41237 (2015). doi: 10.1002/app.41237.
28. L.Y. Mwaikambo and M.P. Ansell, The determination of porosity and cellulose content of plant fibers by density methods. *J. Mater. Sci. Lett.* **20**, 2095–2096 (2001). doi: 10.1023/A:1013703809964.
29. L. Segal, J.J. Creely, A.E. Martin Jr., and C.M. Conrad, An empirical method for estimating the degree of crystallinity of native cellulose using the X-ray diffractometer. *Text Res. J.* **29**, 64–786 (1959). doi: 10.1177/004051755902901003.
30. ASTM E96-95, Standard test methods for water vapour transmission of materials. In Annual Book of ASTM Standards American Society for Testing and Materials, Philadelphia (1995).
31. ASTM D 3985-10, Standard test method for oxygen gas transmission rate through plastic film and sheeting using a colorimetric sensor. In Annual Book of ASTM Standards American Society for Testing and Materials, Philadelphia (2010).
32. Z. Yan, S. Chen, H. Wang, B. Wang, C. Wang, and J. Jiang, Cellulose synthesized by Acetobacter xylinum in the presence of multi-walled carbon nanotubes. *Carbohydr. Res.* **343**, 73–80 (2008). doi: 10.1016/j.carres.2007.10.024.
33. S. Borysiak and J. Garbarczyk, Applying the WAXS method to estimate the supermolecular structure of

cellulose fibres after mercerisation. *Fibres & Text* **11**, 104–106 (2003).
34. H. Jin, C. Zha, and L. Gu, Direct dissolution of cellulose in NaOH/thiourea/urea aqueous solution. *Carbohydr. Res.* **342**, 851–858 (2007). doi: 10.1016/j.carres.2006.12.023.
35. A. Retegi, N. Gabilondo, C. Peña, R. Zuluaga, C. Castro, P. Gañan, K. de la Caba, and I. Mondragon, Bacterial cellulose films with controlled microstructure-mechanical property relationships. *Cellulose* **17**, 661–669 (2010). doi 10.1007/s10570-009-9389-7.
36. M. Alexandre and P. Dubois, Polymer-layered silicate nanocomposites: Preparation, properties and uses of a new class of materials. *Mat. Sci. Eng.* **28**, 1–63 (2000). doi: 10.1016/S0927-796X(00)00012-7.
37. S. Tunç and O. Duman, Preparation and characterization of biodegradable methyl cellulose/montmorillonite nanocomposite films. *Appl. Clay Sci.* **48**, 414–424 (2010). doi: 10.1016/j.clay.2010.01.016.
38. S.F. Wang, L. Shen, Y.J. Tong, L. Chen, I.Y. Phang, P.Q. Lim, and T.X. Liu, Biopolymer chitosan/montmorillonite nanocomposites: Preparation and characterization. *Polym. Degrad. Stab.* **90**, 123–131 (2005). doi: 10.1016/j.polymdegradstab.2005.03.001.
39. D.R. Ruka, G.P. Simon, and K.M. Dean, In situ modifications to bacterial cellulose with the water insoluble polymer poly-3-hydroxybutyrate. *Carbohydr. Polym.* **92**, 1717–1723 (2013). doi: 10.1016/j.carbpol.2012.11.007.
40. M.I.G. Miranda, C.I.D. Bica, S.M.B. Nachtigall, N. Rehman, and S.M.L. Rosa, Kinetical thermal degradation study of maize straw and soybean hull celluloses by simultaneous DSC–TGA and MDSC techniques. *Thermochim. Acta* **565**, 65–71 (2013). doi: 10.1016/j.tca.2013.04.012.
41. J. George, K.V. Ramana, A.S. Bawa, and Siddaramaiah, Bacterial cellulose nanocrystals exhibiting high thermal stability and their polymer nanocomposites. *Int. J. Biol. Macromol.* **48**, 50–57 (2011). doi: 10.1016/j.ijbiomac.2010.09.013.
42. S.S. Ray and M. Okamoto, Biodegradable polylactide and its nanocomposites: Opening a new dimension for plastics and composites. *Macromol. Rapid. Commun* **24**, 815–840 (2003). doi: 10.1002/marc.200300008.
43. J.M. Yeh, S.J. Liou, M.C. Lai, Y.W. Chang, C.Y. Huang, C.P. Chen, J.H. Jaw, T.Y. Tsai, and Y.H. Yu, Comparative studies of the properties of poly(methyl methacrylate)–clay nanocomposite materials prepared by in situ emulsion polymerization and solution dispersion. *J. Appl. Polym. Sci.* **94**, 1936–1946 (2004). doi: 10.1002/app.21095.
44. C. Aulin, G. Salazar-Alvarez, and T. Lindström, High strength, flexible and transparent nanofibrillated cellulose–nanoclay biohybrid films with tunable oxygen and water vapor permeability. *Nanoscale* **4**, 6622–6628 (2012). doi: 10.1039/c2nr31726e.